Multirate Sampling Method for Acceleration Control System

Mariko Mizuochi, Toshiaki Tsuji, *Member, IEEE*, and Kouhei Ohnishi, *Fellow, IEEE*

***Abstract*—This paper focuses on the realization of high-performance motion control based on acceleration control. A disturbance observer is used to construct an acceleration control system. A high sampling frequency is known to be effective for improving the performance. Characteristics of acceleration control are investigated to discuss the relationship between the performance and a sampling frequency of the system. The needs for a high sampling frequency for an output are then described. Based on these considerations, a novel multirate sampling method for the acceleration control system is proposed. An output sampling period is set shorter than an input sampling period, and control calculation is executed at each output sampling period in the method. The disturbance observer is redesigned for application to the multirate system. Stability analysis is performed to verify the validity of the proposal. Feasibility of the proposed method and its influence on the performance are also verified by experimental results.**

***Index Terms*—Acceleration control, disturbance observer, motion control, multirate control.**

I. Introduction

MOTION control is one of the most important elements for industrial application of robot control. Due to recent rapid progress in robotics, the requirement for complicated motions has been increasing. The more complicated the motion becomes, the more robustness and quicker response are required. Acceleration control gives acceleration reference and makes the system realize desired acceleration. It enables the acquisition of higher robustness compared to control using only position or velocity. Acceleration control also makes it possible to treat force and position in the same dimension. For these reasons, acceleration control is inevitable for motion control. As an effective tool to realize robust acceleration control, a disturbance observer [1] has been proposed. It estimates disturbance torque in an acceleration dimension and compensates it.

Robotic systems are often controlled in discrete time, and a controller designed for continuous-time systems (analog) is often converted into that for discrete-time systems (digital) by using zero-order hold (ZOH) technique. Shortening a sampling period is effective in widening the bandwidth in which acceleration control is realized [2]. A high sampling frequency therefore enables the acquisition of better performance. On the other hand, sampling periods have limitations relating to hardware performances even with recent dramatic development of hardware. The calculation time of a computer, processing times of a counter and an analog-to-digital or digital-to-analog converter, frequency of pulsewidth modulation (PWM), and processing rates of sensors can be mentioned as examples. In general, one constant sampling period is selected for input $(u(t))$, output $(y(t))$, and controller $(r(t))$. In this paper, "input" is defined as input torque or the current to a controlled object. "Output" is then defined as the information of a controlled object, such as position or force, acquired with sensors. Due to limitations of sampling periods, the sampling period for a system is selected so as to be equal to the longest of those three. On the other hand, sampling periods are set individually in multirate sampling control [3]. As a result, better performance can be acquired despite hardware limitations. Many studies have been performed on the system in which output information cannot be acquired fast enough, such as computer hard disk drives or visual servo systems [4]–[6]. The methods interpolate the output information with a focus on the state between sampling points and update the actuation input at a shorter sampling period. Many control systems, however, have more severe limitation on an input sampling period than on an output. In motor control, output information is mainly acquired from optical encoders. It can be acquired in proportion to the clock time of a field-programmable gate array (FPGA) or digital signal processor. On the other hand, a frequency of a current input is limited by the performance of an amplifier or frequency of PWM and cannot be heightened even with a new device such as an FPGA. An output sampling period can be therefore set shorter than an input in many cases. There are only a few research in which an output sampling period is set shorter than an input. An example is the proposal of using it for a utility interactive inverter focusing on behavior during the sampling period, which is not compensated in deadbeat control [7]. Multirate sampling control methods are also utilized to save computation and to change sampling periods among controllers [8], [9].

An aim of this paper is the realization of acceleration control in wide bandwidth. This paper focuses on the relationship between the performance and the sampling frequency of acceleration control. The needs of a higher sampling frequency for an output than for an input are described. From this point of view,

Manuscript received December 28, 2005; revised July 31, 2006. Abstract published on the Internet January 27, 2007.

M. Mizuochi and K. Ohnishi are with the Department of System Design Engineering, Keio University, Yokohama 223-8522, Japan (e-mail: mariko@sum.sd.keio.ac.jp; ohnishi@sd.keio.ac.jp).

T. Tsuji is with the Department of Mechanical Engineering Faculty of Engineering Division I, Tokyo University of Science, Tokyo 162-8602, Japan (e-mail: tsuji@kobalab.com).

Color versions of one or more of the figures in this paper are available online at http://ieeexplore.ieee.org.

Digital Object Identifier 10.1109/TIE.2007.893002

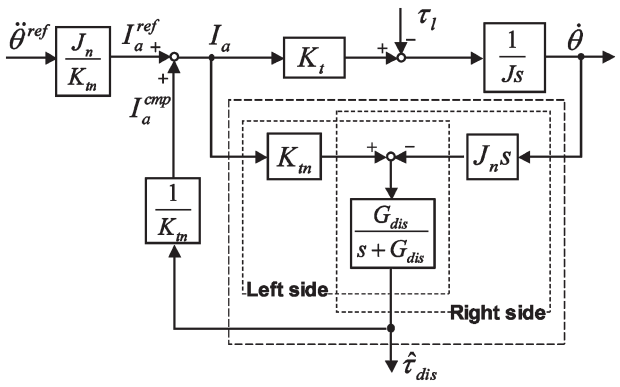

Fig. 1. Disturbance observer.

this paper proposes a novel multirate sampling method with a shorter output sampling period. The disturbance observer is redesigned to fit to the multirate system with a new definition of disturbance torque. Shimada *et al.* [7] used the output information acquired in a short sampling period only to correct the input value. It is utilized, however, not only for correction but also for the overall controller in the proposed method. As a result, the performance becomes close to that of the system that has a short sampling period for both an output and an input. Stability analysis is performed to make a comparison with single-rate control and to verify the validity of the proposal. Experimental results with both high- and low-resolution encoders support the feasibility of the proposed method. Although the method can be applied to various systems, analysis and experiments are carried out with a single-input–single-output system to simplify the discussion.

II. Acceleration Control

In this section, characteristics of acceleration control are discussed focusing on its sampling periods. Fig. 1 shows the block diagram of the disturbance observer. In this paper, τ_l denotes the mechanical load, $\hat{\tau}_{\rm dis}$ denotes the estimated disturbance torque, $G_{\rm dis}$ denotes the cutoff frequency of the disturbance observer, $I_a^{\rm ref}$ denotes the current reference, K_t denotes the torque constant, J denotes the inertia, s denotes the Laplace variable, and the subscript n denotes the nominal value. This paper assumes that the current minor loop in the motor driver is fast enough to treat the current reference as the real current input.

The total disturbance torque $\tau_{\rm dis}$ contains the mechanical load τ_l, the varied self-inertia torque $\Delta J\ddot{\theta}$, and the torque ripple from the motor $\Delta K_t I_a^{\rm ref}$ and is given as

$$\tau_{\rm dis} = \tau_l + \Delta J\ddot{\theta} - \Delta K_t I_a^{\rm ref}. \tag{1}$$

Disturbance torque is calculated by the following equation:

$$\tau_{\rm dis} = K_{tn} I_a^{\rm ref} - J_n \dot{\theta} s. \tag{2}$$

The first term $K_{tn} I_a^{\rm ref}$ in (2) is based on input information, and the second term $J_n \dot{\theta} s$ is based on output information. In other words, the first corresponds to the left side of the disturbance observer in Fig. 1, whereas the second corresponds to the right side. The estimated disturbance torque is obtained through a low-pass filter (LPF), considering derivative calculation in the second term and is given as

$$\hat{\tau}_{\rm dis} = \frac{G_{\rm dis}}{s + G_{\rm dis}} \left(K_{tn} I_a^{\rm ref} - J_n \dot{\theta} s \right). \tag{3}$$

The introduction of the disturbance observer realizes acceleration control and improves robustness of the system. In fact, the robustness is not assured in the frequency range higher than the cutoff frequency of the disturbance observer $G_{\rm dis}$. The cutoff frequency can be set higher by shortening a sampling period [2].

Generally, the data acquired in experimental systems are mainly angular information from a rotary encoder. Disturbance estimation in the disturbance observer is based on the acceleration $\dot{\theta} s$. Thus, derivative calculation is performed twice in the right side. Since it is usually difficult in experiments to use a derivative value directly due to data noise mainly derived from a quantization error of the encoder, pseudoderivative calculation with an LPF is often introduced. The velocity is calculated as follows:

$$\hat{\dot{\theta}} = s \frac{G_v}{s + G_v} \theta \tag{4}$$

where G_v denotes the cutoff frequency of the LPF. It means that two LPFs are introduced into the right side of the disturbance observer to realize acceleration control, considering pseudoderivative and the disturbance observer. Since the data acquired through an LPF are delayed, acceleration information in the second term of (2) calculated from angular data is delayed compared to the current reference in the first term. It is better to reduce the delay by acquiring output information in a shorter sampling period than to input delayed values at a high rate. In other words, it is preferable to acquire the output information at a rate higher than the renewal rate of an actuation input to minimize the delay.

III. Multirate Sampling

A. Multirate Sampling Method for Acceleration Control

This section proposes a new multirate sampling method for the acceleration control system. Here, output and input periods are defined as follows:

- output sampling period: sampling period for acquisition of sensor information;
- input sampling period: sampling period for renewal of a current input reference.

As mentioned in the previous section, it is important in acceleration control systems to acquire output information in a sampling period shorter than that for renewal of an actuation input. The authors therefore propose a new multirate sampling method, shown in Fig. 2, in which output information is acquired several times during one input sampling period. The sampling period of an input T_u and that of the controller T_r are selected to satisfy the following equations:

$$T_u = nT_y \tag{5}$$

$$T_r = T_y \tag{6}$$

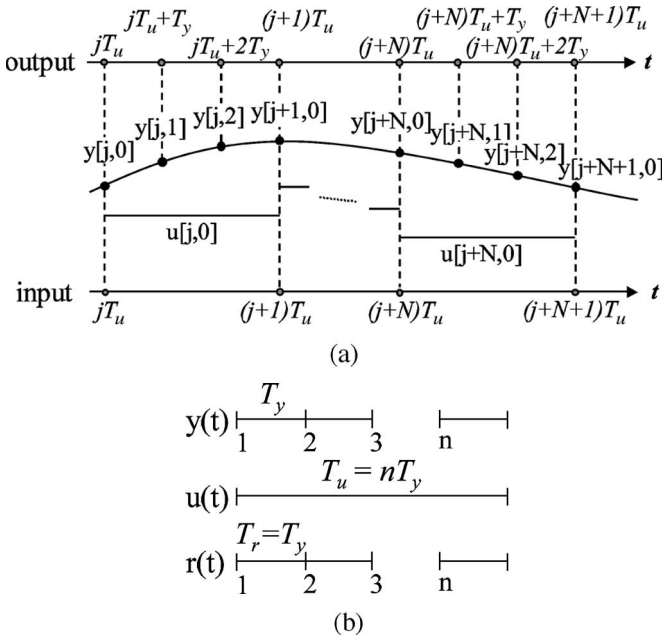

Fig. 2. Multirate sampling method for acceleration control. (a) Multirate sampling. (b) Sampling periods.

where T_y is the output sampling period, and n is the integer number. Control calculation is therefore performed at each output sampling period. Here, the controller includes all items that decide the input value, such as observers.

The limitations on sampling periods also support the adequacy of the proposal. The limitations on the input sampling period are generally more severe than those on the output. An output sampling period can be selected in proportion to the clock time of the DSP or FPGA. A control sampling period is limited only by calculation time. Those sampling periods can be shortened with the development of devices such as an FPGA. On the other hand, a frequency of a current input is limited strictly by the performance of an amplifier or a frequency of PWM. Therefore, the output sampling period can be set shorter than the input in many cases.

Consider a continuous-time plant represented as follows:

$$\dot{\boldsymbol{x}}(t) = \mathbf{A}\boldsymbol{x}(t) + \boldsymbol{b}u(t) \tag{7}$$

$$y(t) = \boldsymbol{c}\boldsymbol{x}(t). \tag{8}$$

Assuming that the sampling periods of output and input are T, and the input $u(\tau)$ remains constant from t_0 to $t_0 + T$, the discrete-time plant is represented as follows:

$$\boldsymbol{x}[i+1] = \mathbf{A}_d\boldsymbol{x}[i] + \boldsymbol{b}_d u[i] \tag{9}$$

$$\boldsymbol{y}[i] = \boldsymbol{c}_d^T\boldsymbol{x}[i] \tag{10}$$

where $\boldsymbol{x}[i] = \boldsymbol{x}(iT)$. Matrix $\mathbf{A}_d$ and vectors $\boldsymbol{b}_d$ and $\boldsymbol{c}_d$ are given by

$$\mathbf{A}_d = e^{\mathbf{A}T}, \quad \boldsymbol{b}_d = \int_0^T e^{\mathbf{A}\tau}d\tau\boldsymbol{b}, \quad \boldsymbol{c}_d = \boldsymbol{c}.$$

When a feedback control law is $u(t) = f(\boldsymbol{x}(t))$, it is rewritten as $u[i] = f(\boldsymbol{x}[i])$ in discrete time.

In the proposed method, since the actuation input is updated only when $t = iT_u$ (i: integer number), the feedback control law in the multirate system is given by the following equation:

$$u[i,k] = u[i,0] = f\left(\boldsymbol{x}[i,0]\right). \tag{11}$$

This equation shows that the actuation input remains constant from $t = iT_u$ to $t = (i+1)T_u$. In the proposed multirate method, the state-space (9) and (10) can therefore be rewritten into the following equations, considering the relation of two sampling periods, T_y and T_u:

$$\boldsymbol{x}[i,k+1] = \mathbf{A}_m\boldsymbol{x}[i,k] + \boldsymbol{b}_m u[i,0] : k \neq n-1 \tag{12}$$

$$\boldsymbol{x}[i+1,0] = \mathbf{A}_m\boldsymbol{x}[i,n-1] + \boldsymbol{b}_m u[i,0] : k = n-1 \tag{13}$$

$$\boldsymbol{y}[i,k] = \boldsymbol{c}_m^T\boldsymbol{x}[i,k] \tag{14}$$

where

$$\boldsymbol{x}[i,k] = \boldsymbol{x}(iT_u + kT_y), \qquad k = 0,\ldots,n-1$$

$$\mathbf{A}_m = e^{\mathbf{A}T_y}, \quad \boldsymbol{b}_m = \int_0^{T_y} e^{\mathbf{A}\tau}d\tau\boldsymbol{b}, \quad \boldsymbol{c}_m = \boldsymbol{c}.$$

B. Disturbance Observer in Multirate System

The application of an observer to multirate systems has been discussed in [11]. It shows just an extension to multirate systems and does not focus especially on the characteristics of the systems with a short output sampling period. The authors therefore focus on the characteristics and present two types of disturbance observers: the extension of the observer with the conventional definition of disturbance torque (1) and a novel disturbance observer for the proposed multirate system with a new definition of disturbance torque.

In the proposed multirate system, there are two values of an input: desired input value $I_m[i,k]$ and real input reference value $I_m^{\mathrm{real}}[i,k]$. The former is calculated at an output sampling rate, and the latter is a real input reference value to the robot, which is renewed at an input sampling rate. From (11), the following relation is obtained:

$$I_m^{\mathrm{real}}[i,k] = I_m[i,0]. \tag{15}$$

The disturbance observer is designed using Gopinath's method [10] in discrete time, since the multirate system is a discrete-time system. In this paper, however, the authors dare to use Laplace variable in figures and equations to make the correspondence of each figure or equation with Fig. 1 or (3) clear.

1) Application of Conventional Disturbance Observer: A conventional disturbance observer is expanded for the multirate system in Fig. 3(a). The disturbance torque defined in the conventional disturbance observer (1) is represented by the following equation in the multirate system:

$$\tau_{\mathrm{dis}}[i,k] = \tau_l[i,k] + \Delta J\ddot{\theta}[i,k] - \Delta K_t I_m^{\mathrm{real}}[i,k]. \tag{16}$$

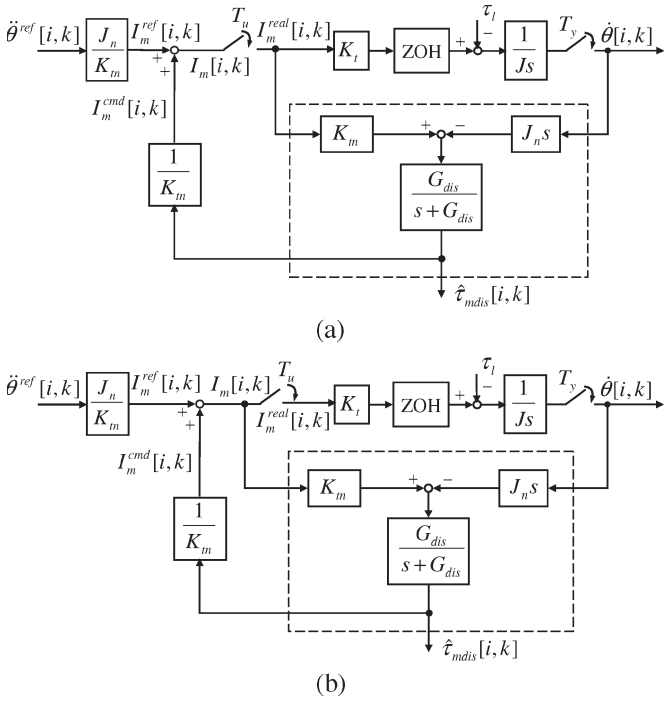

Fig. 3. Disturbance observer in multirate system. (a) Conventional disturbance observer in multirate system. (b) Proposed disturbance observer for multirate system.

The estimated disturbance torque is acquired from the real input reference value $I_m^{\rm real}[i,k]$ and velocity with the following equation:

$$\hat{\tau}_{\rm dis} = \frac{G_{\rm dis}}{s+G_{\rm dis}}\left(K_{tn}I_m^{\rm real}[i,k] - J_n s\dot{\theta}[i,k]\right). \qquad (17)$$

2) Disturbance Observer for Multirate System: Equation (15) shows that there is a deviation between the desired input value and the real input reference value when $t \neq iT_u$. Although the deviation is not considered in the conventional disturbance observer, it may affect the system. With a focus on that, the authors define the total disturbance torque of the multirate sampling system as follows to include the influence of the deviation of the input values:

$$\tau_{\rm mdis}[i,k] = \tau_l[i,k] + \Delta J\ddot{\theta}[i,k] - \Delta K_t I_m[i,k] + (K_{tn}+\Delta K_t)\Delta I_m[i,k] \qquad (18)$$

where

$$\Delta I_m[i,k] = I_m[i,k] - I_m^{\rm real}[i,k].$$

With this definition, the absence of updating an input value, i.e., the influence of an input sampler, is considered as a sort of disturbance. It is expressed in the last term of (18). $I_m[i,k]$ should be used instead of $I_m^{\rm real}[i,k]$ to include the influence of the sampler existing between the desired and real values. The disturbance observer in the multirate system is therefore proposed as shown in Fig. 3(b). The total disturbance torque of the multirate sampling system is estimated by the following equation:

$$\hat{\tau}_{\rm mdis} = \frac{G_{\rm dis}}{s+G_{\rm dis}}\left(K_{tn}I_m[i,k] - J_n s\dot{\theta}[i,k]\right). \qquad (19)$$

C. Application of the Proposed Method

The overall structure of the proposed method is shown in Fig. 4. The following advantages are expected for the proposed multirate sampling method.

- Cutoff frequency can be set higher.
- Information of disturbance is detected in an early timing.

The first advantage is derived from its higher sampling frequency and a larger amount of sampled data for observer calculation. The limitation on the cutoff frequency relates to the sampling period and noise. The short sampling period reduces noise by repeated calculation. The influence of digitization is decreased by shortening the sampling period of the observer. The cutoff frequency can therefore be set higher with a shorter sampling period. The limitation of the cutoff frequency is elevated with the multirate sampling method, since both noise and influence of digitization are reduced. The second advantage is explained with reference to Fig. 5. In the single-rate system, the influence of disturbance $\tau_{\rm dis1}$ exerted at $t = t_1$ and $\tau_{\rm dis2}$ at $t = t_2$ are both recognized at $t = t_0 + T_u$. On the other hand, in the multirate system, the influence of $\tau_{\rm dis1}$ and $\tau_{\rm dis2}$ is recognized at $t_0 + T_y$ and $t_0 + T_u$, respectively. The detection of disturbance influence is generally delayed half an output sampling period on average. When the sampling periods in multirate control satisfy $T_u = nT_y = T_s$, and those in single-rate control satisfy $T_u = T_y = T_s$, the average length of delay is $T_s/2n$ in multirate and $T_s/2$ in single-rate. The average length of delay becomes n times shorter, and the detection becomes early for $(n-1/2n)T_s$ on average with the multirate sampling method. As a result, quick response against disturbance is obtained and the bandwidth of robust acceleration control is increased. On the other hand, the absence of updating of the compensation input that occurs in the proposed method may deteriorate the performance. The proposed disturbance observer enables the system to estimate the disturbance including the influence of the absence of updating. By compensating the value, high performance seems to be obtained. The performance is expected to approach that achieved with a short sampling period for both an output and an input.

IV. Stability Analysis

Stability analysis of both single-rate control and the proposed multirate control is performed to verify the validity of the proposed method. The limitation of the input sampling period is assumed to be 0.1 ms in this analysis. The block diagram of the whole system utilized for the analysis is demonstrated in Fig. 6(a).

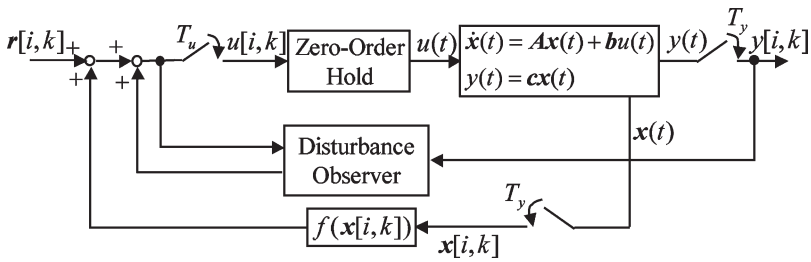

Fig. 4. Multirate control system.

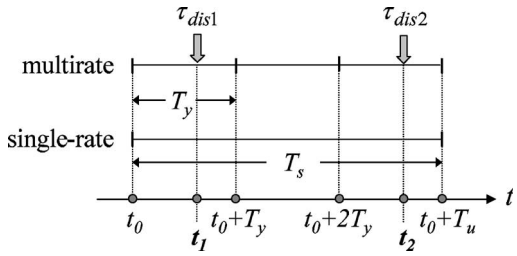

Fig. 5. Disturbance detection.

A. Modeling

A dynamic equation of a one-degree-of-freedom manipulator in discrete time is expressed as follows:

$$\begin{bmatrix} \theta[i+1] \\ \dot{\theta}[i+1] \\ \tau_{\rm dis}[i+1] \end{bmatrix} = \begin{bmatrix} 1 & T & -\frac{T^2}{2J} \\ 0 & 1 & -\frac{T}{J} \\ 0 & 0 & 1 \end{bmatrix} \begin{bmatrix} \theta[i] \\ \dot{\theta}[i] \\ \tau_{\rm dis}[i] \end{bmatrix} + \begin{bmatrix} \frac{T^2}{2J} \\ \frac{T}{J} \\ 0 \end{bmatrix} \tau_m[i] \tag{20}$$

where τ_m denotes the input torque and $\tau_{\rm dis}$ denotes the disturbance torque, which is assumed to be constant between the sampling periods. A PD controller and the disturbance observer are applied to the system. Sampling periods T_u and T_y are set equal in the single-rate control and set to satisfy $T_u = nT_y$ in the multirate control.

1) Single-Rate Control: The state space (20) is expanded to include state variables in the disturbance observer $w_1[i]$ and in pseudo-derivative $w_2[i]$. The disturbance observer is designed based on the Gopinath's method, and pseudoderivative calculation is utilized to acquire velocity from position data. $\boldsymbol{x}[i]$, $u[i]$, $\mathbf{A}_d$, $\boldsymbol{b}_d$, and $\boldsymbol{c}_d$ in (9) are represented as follows:

$$\boldsymbol{x}[i] = [\,\theta[i] \quad \dot{\theta}[i] \quad \tau_{\rm dis}[i] \quad w_1[i] \quad w_2[i]\,]^T$$

$$u[i] = \tau_m[i]$$

$$\mathbf{A}_d = \begin{bmatrix} 1 & T & -\frac{T^2}{2J} & 0 & 0 \\ 0 & 1 & -\frac{T}{J} & 0 & 0 \\ 0 & 0 & 1 & 0 & 0 \\ \hat{b}G_v & 0 & 0 & \hat{a} & \hat{b}G_v(\beta-1) \\ 1 & 0 & 0 & 0 & \beta \end{bmatrix}$$

$$\boldsymbol{b}_d = \begin{bmatrix} \frac{T^2}{2J} & \frac{T}{J} & 0 & \hat{j} & 0 \end{bmatrix}^T$$

$$\boldsymbol{c}_d = [\,1 \quad 0 \quad 0 \quad 0 \quad 0\,]^T$$

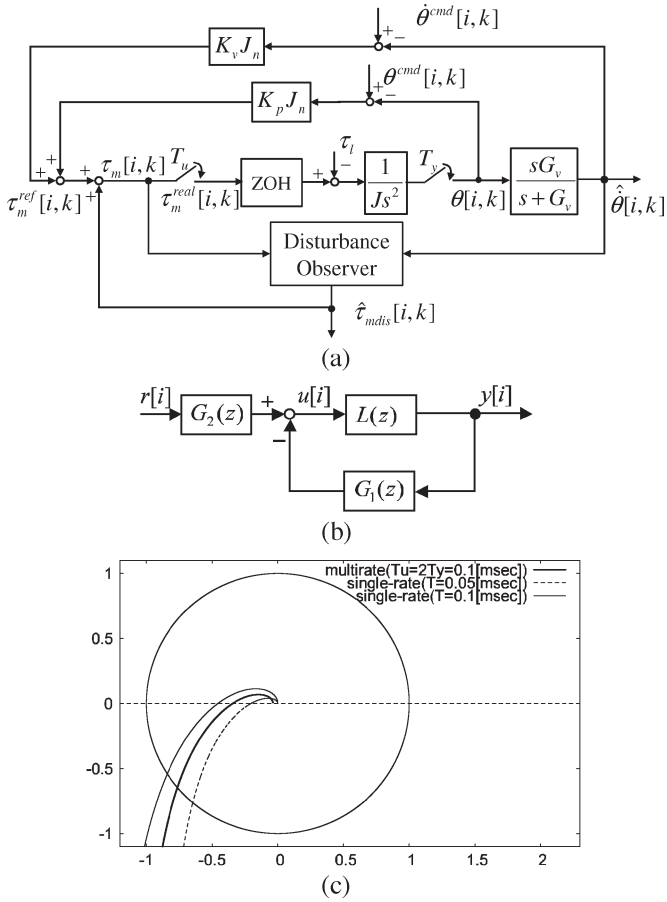

Fig. 6. Model of stability analysis and Nyquist diagram. (a) Analysis model. (b) Structure of system. (c) Nyquist diagram.

where

$$\hat{a} = \alpha, \quad \hat{j} = 1-\alpha, \quad \hat{b} = \frac{J}{T}(1-\alpha)^2,$$
$$\alpha = e^{-G_{\rm dis}T}, \quad \beta = e^{-G_vT}.$$

The velocity calculated with the pseudo-derivative technique and estimated disturbance torque are given by the following equations:

$$\hat{\dot{\theta}}[i] = G_v(\beta-1)w_2[i] + G_v\theta[i] \tag{21}$$

$$\hat{\tau}_{\rm dis}[i] = w_1[i] - l_1\hat{\dot{\theta}} \tag{22}$$

where

$$l_1 = \frac{J}{T}(1-\alpha). \tag{23}$$

The control law is expressed by the following equations:

$$\boldsymbol{w}[i+1] = \hat{\mathbf{A}}\boldsymbol{w}[i] + \hat{\boldsymbol{b}}\theta[i] + \hat{\boldsymbol{j}}\tau_m[i] \tag{24}$$

$$\hat{\boldsymbol{x}}[i] = \hat{\mathbf{C}}\boldsymbol{w}[i] + \hat{\boldsymbol{d}}\theta[i] \tag{25}$$

$$\tau_m[i] = \boldsymbol{k}_d^T\left(\boldsymbol{r}[i] - \hat{\boldsymbol{x}}[i]\right) \tag{26}$$

where

$$\hat{\boldsymbol{x}} = \begin{bmatrix}\theta[i] & \hat{\theta}[i] & \hat{\tau}_m[i]\end{bmatrix}^T$$

$$\boldsymbol{w}[i] = \begin{bmatrix} w_1[i] \\ w_2[i]\end{bmatrix}, \quad \hat{\mathbf{A}} = \begin{bmatrix}\hat{a} & \hat{b}G_v(\beta-1) \\ 0 & \beta\end{bmatrix}$$

$$\hat{\boldsymbol{b}} = \begin{bmatrix}\hat{b}G_v & 1\end{bmatrix}^T, \quad \hat{\boldsymbol{j}} = \begin{bmatrix}\hat{j} & 0\end{bmatrix}^T$$

$$\hat{\mathbf{C}} = \begin{bmatrix}0 & 0 \\ 0 & G_v(\beta-1) \\ 1 & -l_1G_v(\beta-1)\end{bmatrix}$$

$$\hat{\boldsymbol{d}} = \begin{bmatrix}1 & G_v & -l_1G_v\end{bmatrix}^T$$

$$\boldsymbol{k}_d = \begin{bmatrix}K_pJ_n & K_vJ_n & -1\end{bmatrix}^T$$

and $\boldsymbol{r}[i]$ denotes the reference. The following equation is obtained by transforming (24) and (25) into a transfer function expression:

$$\hat{\boldsymbol{x}}[i] = \boldsymbol{k}_y(z)\theta[i] + \boldsymbol{k}_u(z)\tau_m[i]. \tag{27}$$

The transfer functions of the system $L(z)$ and controller $G_1(z)$ in Fig. 6(b) are obtained as follows:

$$L(z) = \boldsymbol{c}_d^T(z\boldsymbol{I} - \mathbf{A}_d)^{-1}\boldsymbol{b}_d \tag{28}$$

$$G_1(z) = \left(1 + \boldsymbol{k}_d^T\cdot\boldsymbol{k}_u\right)^{-1}\boldsymbol{k}_d^T\cdot\boldsymbol{k}_y. \tag{29}$$

2) Multirate Control: The multirate sampling method and the disturbance observer proposed in the previous section are applied to the system. Considering that there are two values of the input torque, the state-space equation is represented as follows:

$$\boldsymbol{x}[i,k+1] = \mathbf{A}_m\boldsymbol{x}[i,k] + \mathbf{B}_m\begin{bmatrix}\tau_m^{\mathrm{real}}[i,k] \\ \tau_m[i,k]\end{bmatrix} \tag{30}$$

$$y[i,k] = \boldsymbol{c}_m^T\boldsymbol{x}[i,k] \tag{31}$$

where

$$\mathbf{A}_m = \mathbf{A}_d, \quad \boldsymbol{c}_m = \boldsymbol{c}_d, \quad T = T_y$$

$$\mathbf{B}_m = \begin{bmatrix}\frac{T^2}{2J} & \frac{T}{J} & 0 & 0 & 0 \\ 0 & 0 & 0 & \hat{j} & 0\end{bmatrix}^T.$$

The input torques are given by the following equations:

$$\tau_m[i,k] = J_n\left(-K_p\theta[i,k] - K_v\hat{\dot{\theta}}[i,k]\right) + \hat{\tau}_{\mathrm{mdis}}[i,k] \tag{32}$$

$$\tau_m^{\mathrm{real}}[i,k] = \tau_m[i,0]. \tag{33}$$

Equation (30) is the state-space equation described for the shorter sampling period, the output sampling period. It is necessary, however, to describe the system for the longer sampling period for analysis. In order to rewrite the system for the longer sampling period, there are two alternatives [12]. In other words, a high-dimensional state space is selected and a set of equations with simple coefficients is obtained, or a low-dimensional state space is selected and a set of equations with more complicated coefficients is obtained. The former method described in [12] is used in this paper. The state vectors are expanded as follows:

$$\boldsymbol{x}_M[i] = \begin{bmatrix}\boldsymbol{x}[i-1,1] \\ \vdots \\ \boldsymbol{x}[i-1,n-1] \\ \boldsymbol{x}[i,0]\end{bmatrix} \quad \boldsymbol{y}_M[i] = \begin{bmatrix} y[i,0] \\ \vdots \\ y[i,n-1]\end{bmatrix}. \tag{34}$$

The expanded reference $\boldsymbol{r}_M[i]$ and control signal $\boldsymbol{\tau}_{mM}[i]$ are defined in parallel to $\boldsymbol{y}_M[i]$. The state-space equations of the expanded system are represented in the following equations:

$$\boldsymbol{x}_M[i+1] = \mathbf{A}_M\boldsymbol{x}[i] + \mathbf{B}_M\boldsymbol{\tau}_{mM}[i] \tag{35}$$

$$\boldsymbol{y}_M[i] = \mathbf{C}_M\left(\mathbf{U}_1\boldsymbol{x}_M[i+1] + \mathbf{U}_2\boldsymbol{x}_M[i]\right) \tag{36}$$

where

$$\mathbf{A}_M = \begin{bmatrix}0 & \cdots & 0 & \mathbf{A}_m \\ \vdots & \ddots & \vdots & \vdots \\ 0 & \cdots & 0 & \mathbf{A}_m^n\end{bmatrix}$$

$$\mathbf{C}_M = \begin{bmatrix}\mathbf{0} & \cdots & \cdots & \mathbf{0} & \boldsymbol{c}_m \\ \boldsymbol{c}_m & \mathbf{0} & \cdots & \cdots & \mathbf{0} \\ \mathbf{0} & \boldsymbol{c}_m & \mathbf{0} & \cdots & \mathbf{0} \\ \vdots & & \ddots & & \vdots \\ \mathbf{0} & \cdots & \cdots & \boldsymbol{c}_m & \mathbf{0}\end{bmatrix}$$

$$\mathbf{B}_M = \begin{bmatrix}\mathbf{B}_0 \\ \mathbf{A}_m\mathbf{B}_0 + \mathbf{B}_1 \\ \vdots \\ \mathbf{A}_m^{n-1}\mathbf{B}_0 + \mathbf{A}_m^{n-2}\mathbf{B}_1 + \cdots + \mathbf{A}_m\mathbf{B}_{n-2} + \mathbf{B}_{n-1}\end{bmatrix}$$

$$\mathbf{B}_p = \begin{bmatrix}\boldsymbol{b}_1 & \cdots & \boldsymbol{b}_{p+1} & \cdots & \boldsymbol{b}_n\end{bmatrix}$$

$$\boldsymbol{b}_1 = \begin{bmatrix}\frac{T^2}{2J} & \frac{T}{J} & 0 & 0 & 0\end{bmatrix}^T$$

$$\boldsymbol{b}_{p+1} = \begin{bmatrix}0 & 0 & 0 & \hat{j} & 0\end{bmatrix}^T$$

$$\boldsymbol{b}_q = \begin{bmatrix}0 & 0 & 0 & 0 & 0\end{bmatrix}^T (q \neq 1, p+1)$$

$$\mathbf{U}_1 = \mathrm{block\ diag}(\mathbf{I}_n, \ldots, \mathbf{I}_n, \mathbf{0})$$

$$\mathbf{U}_2 = \mathrm{block\ diag}(\mathbf{0}, \ldots, \mathbf{0}, \mathbf{I}_n)$$

and the subscript M denotes the expanded matrices. The control law must also be rewritten for the longer sampling period. The expanded variable $\boldsymbol{w}_M[i]$ is defined in parallel to $\boldsymbol{x}_M[i]$, whereas $\hat{\boldsymbol{x}}_M[i]$ is in parallel to $\boldsymbol{y}_M[i]$. The expanded control law is given by the following equations:

$$\boldsymbol{w}_M[i+1] = \hat{\mathbf{A}}_M\boldsymbol{w}_M[i] + \hat{\mathbf{B}}_M\boldsymbol{y}_M[i] + \hat{\mathbf{J}}_M\boldsymbol{\tau}_{mM}[i] \tag{37}$$

$$\hat{\boldsymbol{x}}_M[i] = \hat{\mathbf{C}}_M(z\bar{\mathbf{U}}_1 + \bar{\mathbf{U}}_2)\boldsymbol{w}_M[i] + \hat{\mathbf{D}}_M\boldsymbol{y}_M[i] \tag{38}$$

$$\boldsymbol{\tau}_{mM}[i] = \mathbf{K}_{dM}\left(\boldsymbol{r}_M[i] - \hat{\boldsymbol{x}}_M[i]\right) \tag{39}$$

where

$$\hat{\mathbf{B}}_M = \begin{bmatrix} \hat{\mathbf{B}} & \mathbf{0} & \cdots & \mathbf{0} \\ \hat{\mathbf{A}}\hat{\mathbf{B}} & \hat{\mathbf{B}} & \mathbf{0} & \mathbf{0} \\ \vdots & & \ddots & \\ \hat{\mathbf{A}}^{n-1}\hat{\mathbf{B}} & \hat{\mathbf{A}}^{n-2}\hat{\mathbf{B}} & \cdots & \hat{\mathbf{B}} \end{bmatrix}$$

$$\hat{\mathbf{J}}_M = \begin{bmatrix} \hat{\boldsymbol{j}} & \mathbf{0} & \cdots & \mathbf{0} \\ \hat{\mathbf{A}}\hat{\boldsymbol{j}} & \hat{\boldsymbol{j}} & \mathbf{0} & \mathbf{0} \\ \vdots & & \ddots & \\ \hat{\mathbf{A}}^{n-1}\hat{\boldsymbol{j}} & \hat{\mathbf{A}}^{n-2}\hat{\boldsymbol{j}} & \cdots & \hat{\boldsymbol{j}} \end{bmatrix}$$

$$\hat{\mathbf{D}}_M = \text{block diag}(\hat{\boldsymbol{d}}, \ldots, \hat{\boldsymbol{d}}).$$

The expanded matrices $\hat{\mathbf{A}}_M$, $\hat{\mathbf{C}}_M$, $\mathbf{K}_{dM}$, $\bar{\mathbf{U}}_1$, and $\bar{\mathbf{U}}_2$ are defined in parallel to $\mathbf{A}_M$, $\mathbf{C}_M$, $\hat{\mathbf{D}}_M$, $\mathbf{U}_1$, and $\mathbf{U}_2$, respectively. The following equation is obtained by transforming (37) and (38) into a transfer function expression:

$$\hat{\boldsymbol{x}}_M[i] = \mathbf{K}_{yM}\boldsymbol{y}_M[i] + \mathbf{K}_{uM}\boldsymbol{\tau}_{mM}[i]. \tag{40}$$

The transfer functions of the expanded system $\mathbf{L}(z)$ and controller $\mathbf{G}_1(z)$ are obtained as follows:

$$\mathbf{L}(z) = \mathbf{C}_M(z\mathbf{U}_1 + \mathbf{U}_2)(z\mathbf{I} - \mathbf{A}_M)^{-1}\mathbf{B}_M \tag{41}$$

$$\mathbf{G}_1(z) = (\mathbf{I} + \mathbf{K}_{dM}\mathbf{K}_{uM})^{-1}\mathbf{K}_{dM}\mathbf{K}_{yM}. \tag{42}$$

B. Stability Analysis

Nyquist criterion in continuous-time is obtained by drawing a Nyquist diagram of $\det[\mathbf{I} + \mathbf{L}(z)\mathbf{G}_1(z)] - 1$. The Nyquist diagram of the system is shown in Fig. 6(c). This analysis was performed with the assumption that the limitation of the input sampling period is 0.1 ms. Sampling periods were then set as $T = 0.1$ ms, and $T = 0.05$ ms in single-rate control, and $T_u = 0.1$ ms, $T_y = 0.05$ ms in multirate control. The gains and cutoff frequencies were the same in all cases; $K_p = 900$, $K_v = 60$, $G_v = 13\,000$ rad/s, $G_{\text{dis}} = 700$ rad/s. The result of the proposed method shows a clear improvement of stability compared with that of single-rate control with $T = 0.1$ ms, although it does not come up with the result for $T = 0.05$ ms. Note that the case with $T = 0.05$ ms does not satisfy the assumed limitation. The result indicates that shortening the output sampling period is effective to improve stability, especially when there are limitations on the input sampling period.

V. Experiments

The results of the stability analysis seem to indicate that the shorter the sampling periods are, the higher the stability becomes. The problems involved in shortening the output sampling period are easily conceived, however. One problem is that the shorter output sampling requires more computations. Another is the problem with encoder resolution. In spite of much research on velocity measurement from encoder information [13], a quantization error is not negligible. Although the error is not considered in the stability analysis, it must be taken into account for practical application. Experimental results of the proposed multirate sampling method are demonstrated and compared with those of the single-rate sampling control in this section to show the feasibility and effectiveness.

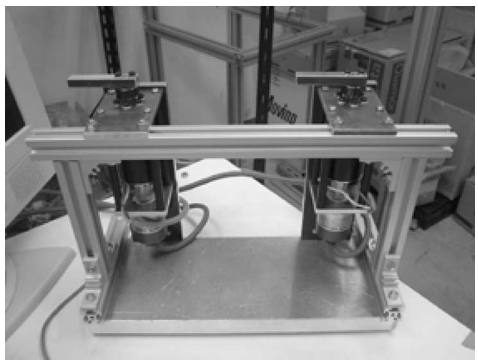

Fig. 7. Experimental equipment.

TABLE I
Encoder and Motor Data

Type of encoder	Canon R-1O
Number of Pulses [pulse/rev]	81,000
Type of encoder	Maxon HEDS 5540
Number of Pulses [pulse/rev]	500
Type of Motor	Maxon RE-40
Torque constant [mNm/A]	60.3

A. Experimental Setup

Experiments were performed with the equipment shown in Fig. 7. The program of the controller is written in C language and implemented under RT-Linux. Specifications of the motor and the encoders are presented in Table I. The pulses of the encoder were multiplied by four in a counter board to improve resolution.

B. Experimental Results

In this experiment, a 0.05-N·m torque disturbance was added as a step input from $t = 7.0$ s to $t = 7.5$ s and $t = 10.5$ s to $t = 11.0$ s while the manipulator was moved as a sine wave. The position and velocity gains were $K_p = 1500$ and $K_v = 100$ in all cases. The cutoff frequency of velocity calculation G_v was set higher than that of the disturbance observer. G_{dis} was then increased to the maximum value with which the system does not significantly oscillate or diverge. Fig. 8 shows the position command and the response. Shaded areas show the response with the disturbance. The experiments were performed under the assumption that the limitation of the input sampling period is 0.3 ms. In order to verify the effects of shortening the output sampling period and of the proposed disturbance observer, four patterns of experiments, listed below, were performed:

- single-rate control with a short sampling period;
- single-rate control with a long sampling period;
- multirate control using the conventional disturbance observer;
- multirate control using the proposed disturbance observer.

Table II presents the sampling periods and the gains in each experiment. Fig. 8(b) and (c) shows the position error when

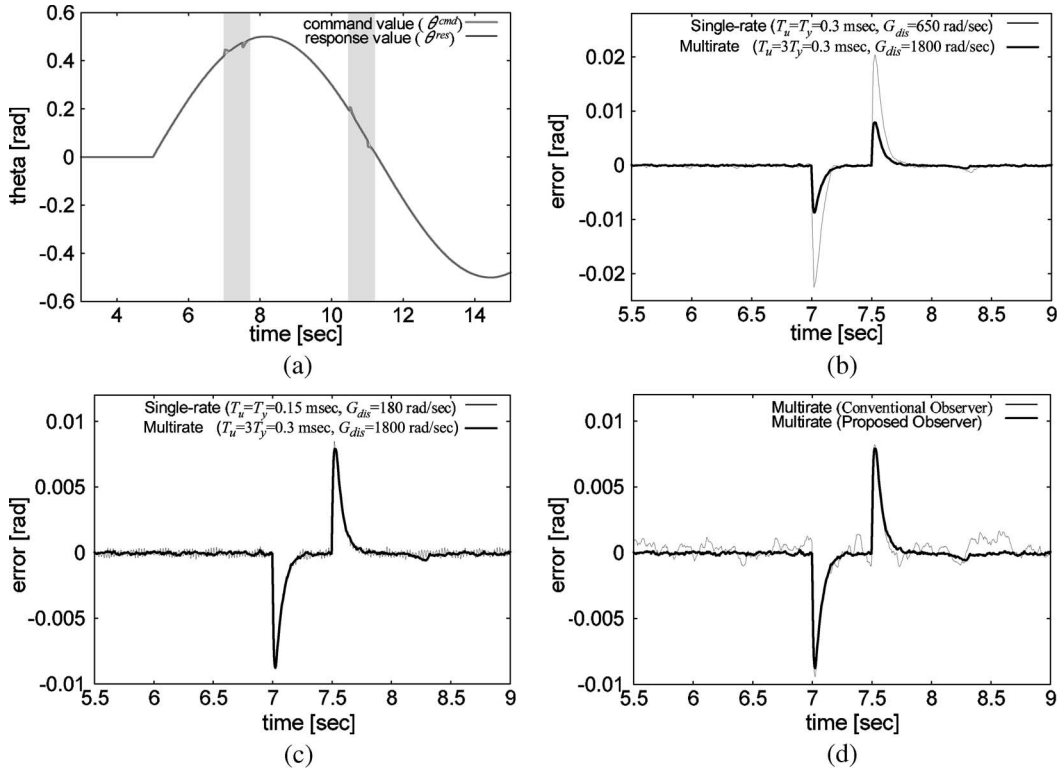

Fig. 8. Experimental results. (a) Position command and response. (b) Comparison of single-rate ($T_u = T_y = 0.3$) and multirate. (c) Comparison of single-rate ($T_u = T_y = 0.15$) and multirate. (d) Comparison of disturbance observers.

TABLE II
CONTROL PARAMETERS IN EXPERIMENTS

	T_y	T_u	G_v	G_{dis}
High Resolution Encoder				
Single-rate ($T_u = T_y = 0.3$)	0.3	0.3	1900	650
Single-rate ($T_u = T_y = 0.15$)	0.15	0.15	2500	1800
Multirate (Conventional Observer)	0.1	0.3	2500	1800
Multirate (Proposed Observer)	0.1	0.3	2500	1800
Low Resolution Encoder				
Single-rate ($T_u = T_y = 0.3$)	0.3	0.3	700	2300
Single-rate ($T_u = T_y = 0.2$)	0.2	0.2	700	3500
Multirate ($T_u = 2T_y = 0.4$)	0.2	0.4	700	3500

the disturbance torque was added. Fig. 8(b) is the comparison between the single-rate and multirate controls with the same input sampling period. In the single-rate control, the manipulator oscillated and became unstable with $G_{\rm dis}$ larger than 700 rad/s, whereas it could be set much higher in the multirate control. The influence of the disturbance was greatly reduced, and convergence was also improved. In order to show the advantage of shortening the output sampling period more clearly, the result of the multirate control is compared with that of the single-rate control with a shorter sampling period in Fig. 8(c). Note that the sampling period of the single-rate control was shorter than the assumed limitation. Although $G_{\rm dis}$ could be set as the same as the multirate control, oscillation was confirmed, which was not confirmed in the multirate control. The result indicates that better performance can be acquired by shortening an output sampling period even with a longer input sampling period.

Fig. 8(d) compares the disturbance observers shown in Fig. 3(a) and (b). Although both of them showed almost the same response to the disturbance, they differed in the response without the disturbance. In the case of the conventional disturbance observer, there was an error in a stationary state. The amount was almost the same as that in the single-rate control with a long sampling period. The fact indicates that the multirate control with the conventional disturbance observer can improve only the maximum value of $G_{\rm dis}$ and does not improve the behavior in a stationary state. This may occur due to the difference of desired and real input values at $t \neq iT_u$. On the other hand, the proposed disturbance observer considers the difference of input values as a sort of disturbance and compensates it. It leads to the improvement in the whole behavior not only in the maximum value of the cutoff frequency, but also in the performance in stationary state. The system therefore approaches the system with a short sampling period for both input and output. The result shows superiority of the proposed disturbance observer.

C. Influence of Input and Output Sampling Periods

Simulations were conducted to verify the influence of input and output sampling periods. An input sampling period was set at 0.6 ms, whereas an output sampling period was decided by varying the ratio of input and output sampling periods n from one to five. The manipulator was moved as a sine wave and a 0.1-N·m torque disturbance was added as a step input from $t = 1.5$ s to $t = 2.3$ s. The cutoff frequency of the disturbance

TABLE III
CONTROL PARAMETER AND rms VALUE

	T_u	T_y	G_{dis}	RMS Value	Rate of RMS
Multirate control					
n=1	0.6	0.6	800	2.21×10^{-2}	1.0
n=2	0.6	0.3	1400	1.27×10^{-2}	0.575
n=3	0.6	0.2	1900	9.39×10^{-3}	0.424
n=4	0.6	0.15	2200	8.14×10^{-3}	0.368
n=5	0.6	0.12	2500	7.42×10^{-3}	0.335
Single-rate control					
	0.6	0.6	800	2.21×10^{-2}	1.0
	0.3	0.3	1600	1.12×10^{-2}	0.505
	0.2	0.2	2300	7.83×10^{-3}	0.353
	0.15	0.15	3100	5.85×10^{-3}	0.264
	0.12	0.12	3800	4.80×10^{-3}	0.217

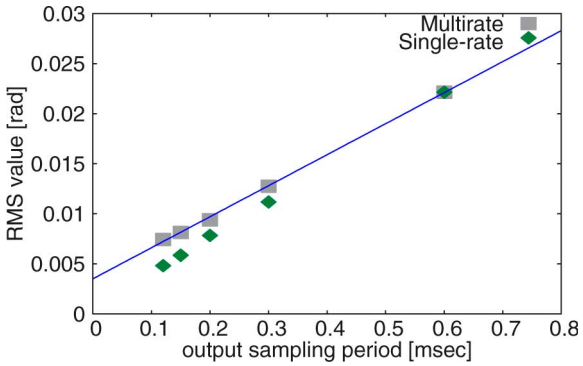

Fig. 9. Relationship of rms values and output sampling period.

observer was increased to the maximum value without large oscillation or divergence, and that of velocity calculation was set as $G_v = 1.2\ G_{\rm dis}$. The root mean square (rms) of the position error from $t = 1.5$ s to $t = 1.9$ s was calculated and compared with that for other cases. The same simulations were conducted for single-rate control. The sampling period was varied from 0.12 to 0.6 ms. Table III presents sampling periods, cutoff frequencies, and rms values. Fig. 9 shows the change of rms values in both multirate and single-rate controls. A line is an approximate curve in multirate control. It shows that the rms value decreases in proportion to an output sampling period, even though an input sampling period was the same in all cases. Comparing the rms values concretely, the value decreases from the single-rate control $(n = 1)$ by 42.47% in $n = 2$ and 66.49% in $n = 5$. These results show that control performance is improved by increasing the ratio n, i.e., shortening an output sampling period. Comparing the single-rate and multirate controls in Fig. 9, the results were better in single-rate control, since input sampling periods were also set as short as output sampling periods. Although the performance of the multirate control could not catch up with that of the single-rate control with a short sampling period, the multirate control follows the single-rate control very well. This shows that the proposed

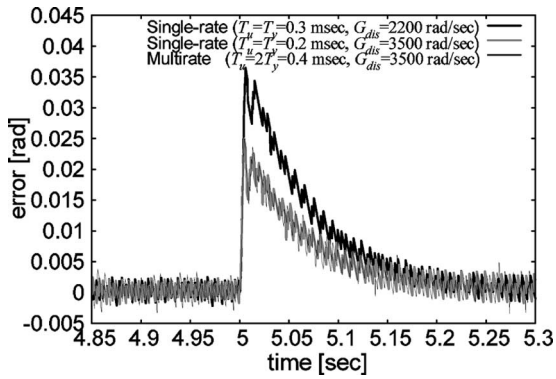

Fig. 10. Experimental results with low-resolution encoder.

method can make the performance close to that with a short sampling period for both input and output. Focusing on the influence of changing sampling periods, the rms value decreases by 63.25% when an input sampling period was 0.6 ms, and an output sampling period was shortened from 0.6 ms to one-fourth, i.e., 0.15 ms. On the other hand, the decrease was only 28.13% when an output sampling period was 0.6 ms, and an input sampling period was shortened to one-fourth, from 0.6 to 0.15 ms. The result shows that the influence of changing an output sampling period is much larger than that of the input. In other words, the sampling period of an output has higher significance than that of an input in acceleration control.

D. Experiments With Low-Resolution Encoder

This subsection applies the proposed method to the system with a low-resolution encoder. The research done in this paper used M method, i.e., fixed-time method for velocity calculation among several measurement methods. The method counts the number of pulses generated in a fixed time interval. Acceleration resolution is in inverse proportion to the square of a sampling period. Since the resolution increases by shortening an output sampling period, the multirate sampling method has a risk to increase the influence of quantization error. In order to verify the applicability of the method to a system with a low-resolution encoder, experiments were performed with an encoder of 500 pulses. The cutoff frequency for velocity calculation was set to $G_v = 700$ rad/s in all cases to keep the influence of a quantization error small. The position and velocity gains were $K_p = 900$ and $K_v = 60$. The sampling periods and gains in each experiment are presented in Table II. In single-rate control, with $T = 0.3$ ms, the system became unstable and diverged with $G_{\rm dis}$ higher than 3000. The maximum value of $G_{\rm dis}$ was the same in single-rate control with $T = 0.2$ ms and multirate control: $G_{\rm dis} = 4500$ rad/s. As a result, the position error when the disturbance torque was added became small in multirate control, as shown in Fig. 10. The noise confirmed in Fig. 10 is due to the low resolution of the encoder and does not mean oscillation of the equipment. Even though an input sampling period was longer in the multirate control, the result was almost the same as that of the single-rate control with a short sampling period. These results show applicability of the proposed method even to the system with a low-resolution

encoder. It is also effective to conduct the proposed method using other measurement methods in case the resolution is extremely low.

VI. Conclusion

This paper has shown higher significance of the sampling period of an output than that of an input in acceleration control. From this point of view, the multirate sampling method for the acceleration control system was proposed. Effectiveness of the proposal was confirmed both in terms of stability and performance. The Nyquist diagram showed improvement in stability by the proposed method. Considering all the experimental results, the advantage of shortening the output sampling period is that better performance can be acquired even with a longer input sampling period. The proposed disturbance observer enables the system to have almost the same performance as a system with a short sampling period not only for the output, but also for the input.

References

[1] K. Ohnishi, M. Shibata, and T. Murakami, "Motion control for advanced mechatronics," *IEEE/ASME Trans. Mechatronics*, vol. 1, no. 1, pp. 56–67, Mar. 1996.

[2] I. Godler, H. Honda, and K. Ohnishi, "Design guidelines for disturbance observer's filter in discrete time," in *Proc. IEEE Int. Workshop Adv. Motion Control*, 2002, pp. 390–395.

[3] M. C. Berg, N. Amit, and J. D. Powell, "Multirate digital control system design," *IEEE Trans. Autom. Control*, vol. 33, no. 12, pp. 1139–1150, Dec. 1988.

[4] T. Hara and M. Tomizuka, "Performance enhancement of multi-rate controller for hard disk drives," *IEEE Trans. Magn.*, vol. 35, no. 2, pp. 898–903, Mar. 1999.

[5] H. Fujimoto and Y. Hori, "Visual servoing based on intersample disturbance rejection by multirate sampling control," in *Proc. IEEE Conf. Decis. and Control*, 2001, pp. 334–339.

[6] H. Fujimoto, Y. Hori, and A. Kawamura, "Perfect tracking control based on multirate feedforward control with generalized sampling periods," *IEEE Trans. Ind. Electron.*, vol. 48, no. 3, pp. 636–644, Jun. 2001.

[7] E. Shimada, K. Aoki, T. Komiyama, and T. Yokoyama, "Implementation of deadbeat control for single phase utility interactive inverter using FPGA," in *Proc. Int. Power Electron. Conf.*, 2005.

[8] M. Tomizuka, "Multi-rate control for motion control application," in *Proc. IEEE Int. Workshop Adv. Motion Control*, 2004, pp. 21–29.

[9] O. Khatib, "A unified approach for motion and force control of robot manipulators: The operational space formulation," *IEEE J. Robot. Autom.*, vol. RA-3, no. 1, pp. 43–53, Feb. 1987.

[10] B. Gopinath, "On the control of linear multiple input-output systems," *Bell Syst. Tech. J.*, vol. 50, no. 3, pp. 1063–1081, 1971.

[11] H. Fujimoto, A. Kawamura, and M. Tomizuka, "Generalized digital redesign method for linear feedback system based on N-delay control," *IEEE/ASME Trans. Mechatronics*, vol. 4, no. 2, pp. 101–109, Jun. 1999.

[12] M. Araki and K. Yamamoto, "Multivariable multirate sampled-data systems: State-space description, transfer characteristics, and nyquist criterion," *IEEE Trans. Autom. Control*, vol. AC-31, no. 2, pp. 145–154, Feb. 1986.

[13] T. Ohmae, T. Matsuda, K. Kamiyama, and M. Tachikawa, "A microprocessor-controlled high-accuracy wide-range speed regulator for motor drives," *IEEE Trans. Ind. Electron.*, vol. IE-29, no. 3, pp. 207–212, Aug. 1982.

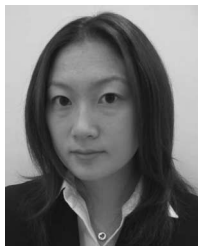

Mariko Mizuochi received the B.E. degree in system design engineering and the M.E. degree in integrated design engineering from Keio University, Yokohama, Japan, in 2004 and 2006, respectively.

Her research interests include motion control, multirate control, and bilateral control.

Toshiaki Tsuji (S'05–M'06) received the B.E. degree in system design engineering and the M.E. and Ph.D. degrees in integrated design engineering from Keio University, Yokohama, Japan, in 2001, 2003, and 2006, respectively.

He is currently a Research Associate at Tokyo University of Science, Tokyo, Japan. His research interests include robotics, motion control, decentralized control, and haptics.

Kouhei Ohnishi (S'78–M'80–SM'00–F'01) received the B.E., M.E., and Ph.D. degrees in electrical engineering from the University of Tokyo, Tokyo, Japan, in 1975, 1977, and 1980, respectively.

Since 1980, he has been with Keio University, Yokohama, Japan. His research interests include robotics, motion control, and haptics.